Journal of Porous Materials
https://doi.org/10.1007/s10934-022-01231-3

Synthesis of light weight recron fiber-reinforced sodium silicate based silica aerogel blankets at an ambient pressure for thermal protection

Sapna B. Jadhav[1,3] · Arwa Makki[2] · Dina Hajjar[2] · Pradip B. Sarawade[1]

Accepted: 1 March 2022

Abstract
In this work, for the sake of improving the performance of homogeneous and flexible silica aerogel blankets in practical applications, lightweight recron fibers were added in silica sol for the fabrication of silica aerogel blankets. The recron based silica aerogel blanket (RSAB) was synthesized by using a low-cost industrial grade sodium silicate precursor with the superficial sol–gel process via ambient pressure drying technique. The as-synthesized RSAB features excellent flexibility, hydrophobic, thermally stable, and mechanical robustness. The Si–C–H bond percentage is maintained at 6% after heat treatment at 270 °C, which results in the high water-repelling phenomenon at a contact angle of 120°. The thermal stability of the aerogel blanket is also confirmed (246 °C) by differential scanning calorimetry. Moreover, the prepared aerogel acquires 87% porosity with homogeneous microstructure and BET surface area as 644 m^2/g. The oxidation peak is detected at 280 °C of $–CH_3$ groups. The latter endowed the RSAB exhibits superior thermal insulation property as well as excellent flexibility. These prepared RSAB aerogel composites may have great integrity for a wide diversity of energy-saving applications. Such RASB can have great potential in electrical appliances for energy conservation purposes due to its lightweight, thermally stable, mechanically robust, highly flexible, and economical manufacturing processes.

Keywords Industrial grade sodium silicate · Monolithic and robust silica aerogel blanket · Recron fiber · Ambient pressure drying · Porosity · Thermal stability · And flexibility

1 Introduction

Nanoporous materials such as aerogels have been appealed for wide-ranging attention in various technical fields for an excessive range of applications [1, 2]. Lightweight nanocomposite has great market integrity in various fields like building construction sectors, automobile industries, and spacecraft applications compared to the traditional inorganic insulation materials like thermocol, and polyester etc. Recently, the acoustic building is the sector in which large amounts of electric energy are consumed due to electrical appliances such as electric heaters, refrigerators, microwaves, and air conditioning systems. With the help of efficient panels of highly thermal insulating materials in electrical appliances and acoustic buildings is a realistic solution of energy demand as a consequence of minimized energy losses. Amongst the variety of aerogels, silica aerogels, are one of the widely used as excellent thermal insulators due to the larger open pore network structure, low thermal conductivity, highly porous nature, and large specific surface areas [3, 4]. Due to the latent and better performance of as a thermal insulator significant attention has been interested by aerogel blankets for their great market outlook in various sectors like building constructions, acoustic insulation, aerospace, aircraft, chemical engineering [5–8]. However, they are integrally fragile ascribed to their weak pearl-like assembly, which restricts their real-world application. Due to shortcoming this short of pure silica aerogel can not be applied as thermal insulation materials are enormously limited by their fragile and low mechanical strength [9]. However, due to the weak mechanical performance, high porosity, and mesoporous nature the commercial application of pure silica aerogel can be the main concern.

✉ Pradip B. Sarawade
pradip.sarawade@physics.mu.ac.in

[1] Department of Physics, University of Mumbai, Kalina, Mumbai 400098, India

[2] Department of Biochemistry, College of Science, University of Jeddah, Jeddah 80327, Kingdom of Saudi Arabia

[3] SDSM College, University of Mumbai, Palghar 401404, India

Published online: 10 March 2022

To overwhelm these limitations, numerous studies have been activated to improve the mechanical strength of silica aerogel with other materials. Initially, researchers reported the strengthening of wet silica gels by aging for a prolonged-time period and heat treatment resulted in minimized shrinkage with the improved mechanical strength of the aerogel manufactured by the supercritical drying method [10–12]. These methods enhanced the degree of polymerization and showed the strength of the silica network backbone. However, such silica aerogels by these approaches were not sufficient for large-scale applications. Presently, several researchers improved the performance of silica aerogel by various strategies including internal strengthening and embedding various inorganic and organic fibers such as carbon nanofibers [13], glass fibers [14, 15], xonotlite fibers [16] and mullite fibers [17] have been reported. Supercritical drying technique (SDT) is the most preferable method for fabricating aerogel over the decades. But SDT requires high pressure and temperature, hindered due to the energy-intensive and cost-ineffectiveness. From a cost-effective, more convenient, and environment-friendly point of view, the ambient pressure drying (APD) method has been actively used as a way for fabricating aerogels [13].

It is familiar that the flexible fibers encourage the development of flexible silica aerogel blankets while increasing the compressive strength of aerogels. However, the density of the blanket, thermal stability, and cost-effective production hindered the contest of enhancing mechanical stability. Therefore, adding lightweight and better thermally stable recron fibers would recover the overall reliability and mechanical stability of the silica aerogel blanket. Silica aerogel blankets, widely reported aerogel developed via tetraethylorthosilicate (TEOS) [16, 18–20] utilized in thermal insulation fields [21–23]. To our knowledge, researchers have yet not reported lightweight fibers-based silica aerogel blankets. Recron fibers have less coming compared to glass fiber, sheep wool, and cotton [24]. In this study, we synthesized a silica aerogel blanket with low cow industrial-grade sodium silicate precursor in comparison to expensive precursors like alkoxides (e.g. TEOS), recron fiber as a filler which is the most abundant and lightweight artificial fiber resource in the world. The recron based silica aerogel blanket (RSAB) was obtained by single-step solvent exchange [13] and surface modification using trimethylchlorosilane (TMCS) as a hydrophobic agent [25, 26] as compared to the lengthy two-step solvent exchange process [27]. The recron fiber embedded into silica aerogel can improve mechanical stability without compromising density, economic production. The purpose of our work was to highlight the thermal stability of lightweight silica aerogel blankets affected by the embedding of recron fibers. The mechanism of efficient panels of highly thermal insulating materials in electrical appliances to conserve energy was also studied and discussed.

In the current work, we employed a highly economic method to develop a monolithic, low density, mechanically strong with high thermally stable recron-based hydrophobic silica aerogel blanket at an ambient pressure drying method. In comparison with other fibers embedded silica aerogel nanocomposite, as prepared RSAB nanocomposite have the density and thermal conductivity, approximately in the range of pure silica aerogels. Owing to the recron fiber themself have a low density (0.89–0.94 g/cm^3), and better tensile strength (350 MPa), which are excellent than that of the other fibers. So the density and mechanical property of the RSAB will not be more affected due to the added recron fibers. On the aspect of better thermal stability than other fibers, added silica aerogel composites are monolithic with improved compressive strength. A 3D silica matrix of the blanket was obtained by embedding a small amount of recron fiber into a silica aerogel matrix. To control the pH of the sol which is the key parameter for the preparation of silica aerogel blanket. Homogeneous distribution of silica particles completely within the fibers obtained by embedding recron fiber into hydrosol before the gelation resulted in formation of homogeneous silica aerogel blanket. The developed aerogel blanket demonstrated reasonable thermal stability and better mechanical robustness due to the uniform distribution of silica particles within the fibers. The internal assembly of the gel can be commendable improved via one step solvent exchange of ethanol/hexane solution during the ambient pressure drying process. A facile hydrophobic agent TMCS can make the aerogel hydrophobic. Furthermore, owing to optimizing the production cost, overcome brittleness with outstanding lightweight thermally stable materials in the field of energy conservation. This sample of silica aerogel blanket is the most convenient material in electrical home appliances against the issue of production of energy with a rapid evaluation of electrical instruments demands of high range energy utilization were also demonstrated.

2 Experimental section

2.1 Materials and methods

For fibrous insulation blankets, the abundantly available lightweight recron fiber has a diameter in the range of 5–20 μm and 5 cm in length with a thickness of the fiber is 0.5 mm is utilized for reinforcement of silica aerogel. The inflated recron fibers are pressed to form the proper size to fit the mold. The chemicals utilized for the synthesis of silica aerogel were industrial grade sodium silicate (Na_2SiO_3) as the main precursor and pure grade chemicals like sulphuric acid (25%, H_2SO_4) were purchased from Romest Silichem Pvt. Ltd. India. Trimethylchlorosilane (> 95%, TMCS) was purchased from Sigma-Aldrich. Other chemicals like

ethanol (EtOH, C_2H_5OH,), and n-hexane (> 99%) were purchased from Duksan chemical. Sulphuric acid (25%, H_2SO_4) (ALDRICH) was used after diluting with deionized water. The recron fibers (5 cm, diameter) were washed with ethanol then dried at 50 °C.

2.2 Preparation of recron fiber reinforced silica aerogels blanket

2.2.1 Preparation of silica hydrosol

The experimental procedure of synthesis of monolithic aerogel blanket is illustrated in Fig. 1 Monolithic silica aerogel blankets were synthesized via a two-step sol–gel polymerization technique. The hydrosol was prepared by using industrial grade sodium silicate (Na_2SiO_3) precursor and acid-catalyzed diluted sulphuric acid (H_2SO_4). Then, the addition of recron fiber before gelation of hydrosol is subsequently followed by solution exchange and surface modification. Final dried blanket obtained with ambient pressure drying process.

Silica hydrosols were prepared by an acid–base catalyzed sol–gel method. Firstly, aq. sulphuric acid (5% H_2SO_4) was added dropwise into the 20 ml of industrial-grade sodium silicate (8% Na_2SiO_3) solutions to control pH to 5 under constant stirring (300 rpm) to execute acid-catalyzed hydrolysis process. The pH of the hydrosol was regulated for condensation by controlling the quantity of H_2SO_4 to retain the gelation time of the hydrosol.

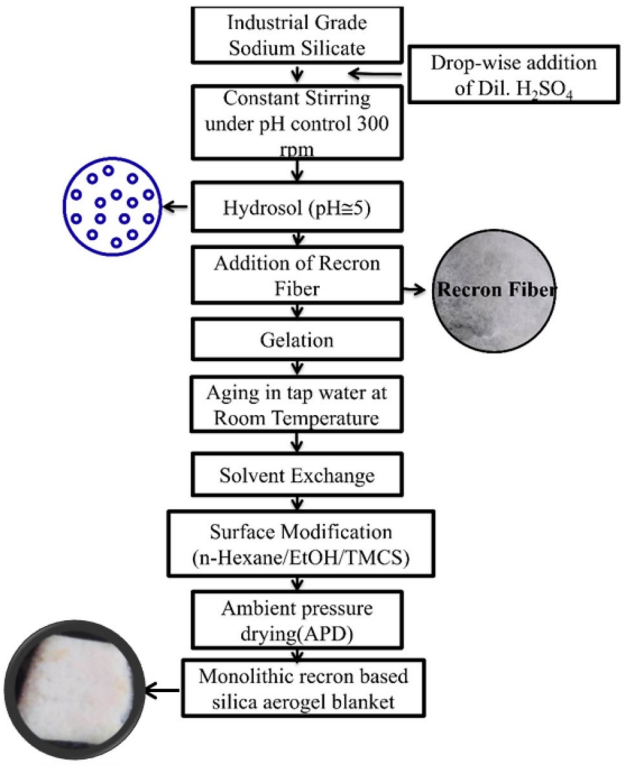

Fig. 1 Flowchart of silica aerogel blanket synthesized using industrial grade sodium silicate solution at an ambient pressure

2.2.2 Preparation of recron fiber-based silica aerogel blanket

Figure 1 depicts the preparation process of RSAB, and the specific steps are as follows: After the formation of uniform hydrosol, a mixture of hydrosol was slowly poured uniformly on the recron fibers (3 wt.%) which were placed in the rectangular mold, to replace the air confined in fiber at room temperature. Then the mold was sealed tightly and kept for gelation. After gelation, mold was kept under continuous running tap water to remove trapped sodium ions from the gel. To further strengthen the gel network, recron added a wet gel blanket that was aged for 6 h into the water at 50 °C. After aging, the mold was kept into the ethanol solvent to exchange the pore fluid (water) which plays a vital role for strengthen the wet gel blanket by preventing shrinkage and cracking of the gel. To maintain three-dimensional silica matrix nanostructures, the wet-gel blanket was immersed in the mixture of polar solvent n-hexane/TMCS/EtOH (volume ration:40:10:50) to drain out water from the silica gel blanket and for a one-step solvent exchange and surface modification processes for 12 h. Immediately the gel turns from transparent to whitish, then slowly turns into light yellow–green precipitate. Afterward, the gel gradually became transparent, indicating the completion of surface modification and solvent substitution of the sample. After a one-step solvent exchange and surface modification processes, a wet-gel blanket was taken out. In the end, surface-modified wet gel blankets were exchanged with n-hexane twice in 12 h to extract the unreacted TMCS silylating agent from the wet gel blanket. For the evaporation of the trapped solvent from the wet gel blanket network to achieve a hydrophobic silica aerogel blanket, a monolithic RSAB sample was kept in the oven at 60 °C for 3 h and then 80 °C for 3 h. For complete removal of the pore fluid finally, the gel was dried at 120 °C for 2 h. After cooling the sample at environmental conditions, various characterization techniques were carried out. Figure 2 reveals a schematic representation of the formation of RSAB with precise stages. Figure 3 represents the schematic overview of recron embedded silica aerogel blanket (RSAB) and its thermal, mechanical, and hydrophobic properties.

2.3 Characterization

The investigation of the influence of reinforcement of recron fiber into the silica hydrosol on various properties of parent samples like packing density, porosity, hydrophobic nature, thermal conductivity, microstructure, and textual properties

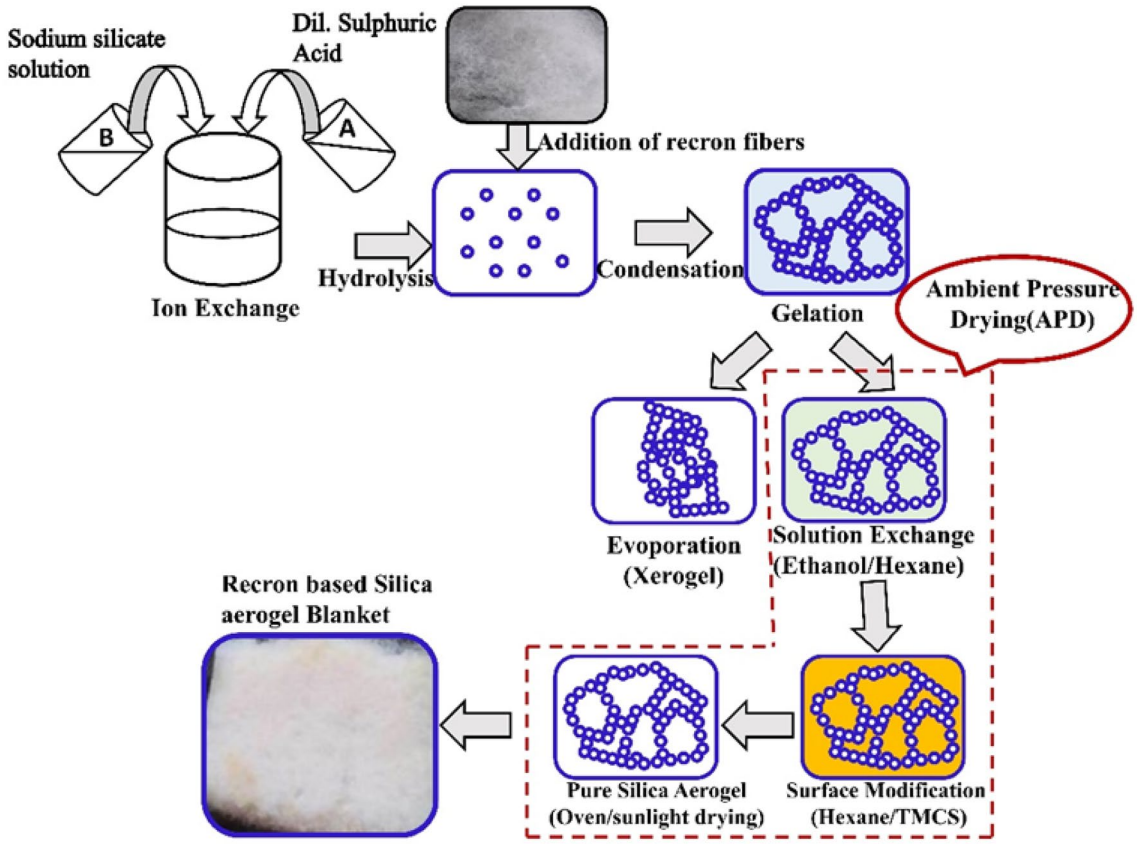

Fig. 2 Schematic representation of preparation of recron reinforced silica aerogel blanket (RSAB)

was investigated using described methods [28]. The bulk density of the monolithic silica aerogel blanket was calculated from the ratio of measurement of the mass of the aerogel by using an electronic micro-balance with an accuracy of up to 10^{-4} g, with the volume of the as-prepared silica aerogel blanket. Each dimension measurement was carried out thrice. The microstructure and morphology of the RSAB were analyzed by field emission Scanning Electron Microscopy (SEM). The average pore diameter (P_d), specific surface area (S_{BET}), and pore volume (P_v) were obtained by the Brunauer–Emmett–Teller (BET) surface area analyzer (Model Micromeritics ASAP 2000). The chemical bonding of the RSAB was characterized by Fourier Transform Infrared (FTIR) spectroscopy using Perkin Elmer (Model number 760). To determine the thermal stability of RSAB samples, in terms of retention of hydrophobicity, samples were examined by thermogravimetric and differential thermal analysis (TG–DTA). The thermal stability and heat capacity (Cp) of RSAB were investigated by using a differential scanning calorimetry (DSC) instrument (SDT Q600). Thermal conductivity study obtained by thermal constant analyzer (TCA). The Universal Testing Machine (UTM) study explored the improved performance of the tensile strength.The hydrophobicity of the aerogel blanket was calculated with a high-resolution DSLR camera where contact angle was measured from water drop placed on the surface of the as synthesized silica aerogel blanket. Porosity (%) of the RSAB was calculated by the equation known below in Eq. (1) [29, 30].

$$\text{Porosity } \% = \frac{(1/\rho b) - (1/\rho s) - (1/\rho f)}{(1/\rho b)} \times 100\ \% \quad (1)$$

In Eq. (1), ρ_f indicates the density of recron reinforced fiber (3 g/cm^3), and ρ_s is the skeletal density of the silica aerogel matrix (2.1 g/cm^3) and ρ_b is the bulk density of the RSAB.

3 Result and discussion

3.1 Porous texture of the silica aerogel blanket

The influence of the addition of recron fiber into silica aerogel on a specific surface was analyzed by N_2 gas adsorption/desorption isotherms of the degassed aerogel sample at

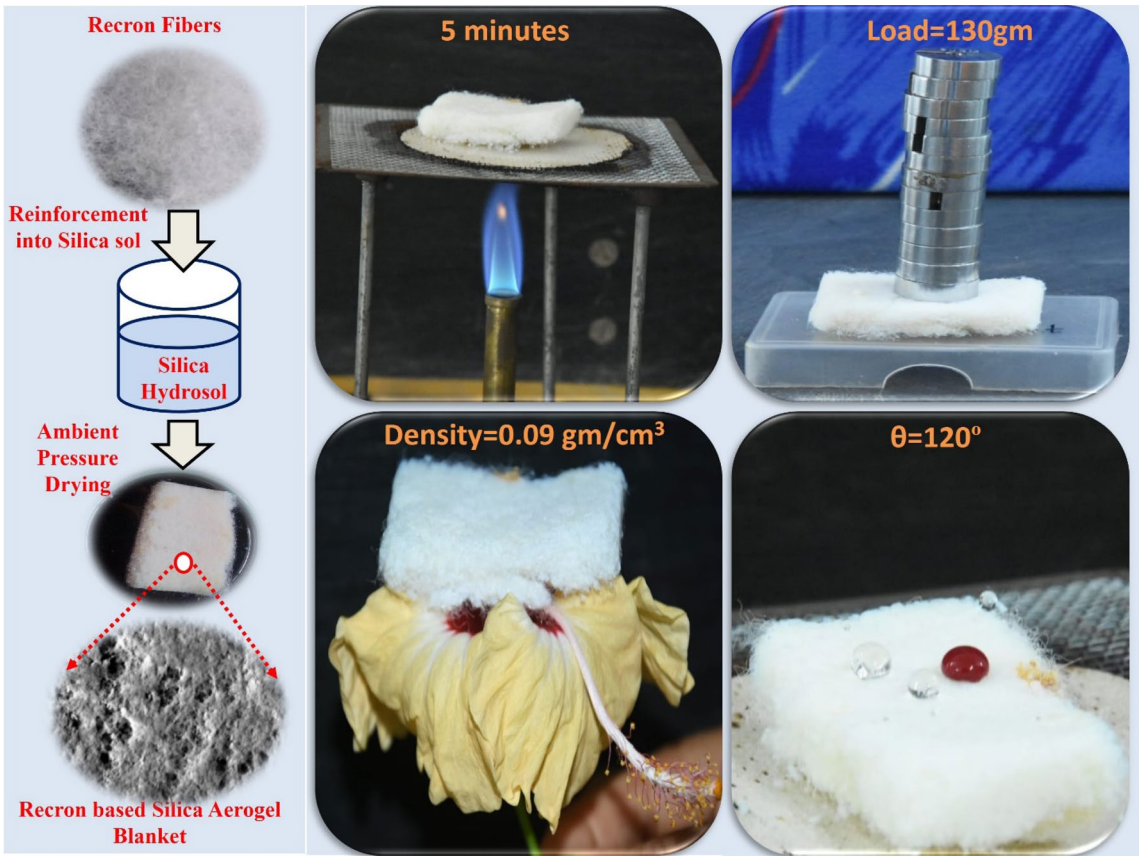

Fig.3 The schematic representation and Photographs of various features **a** Mechanical strength **b** Thermal stability **c** density and **d** hydrophobicity of as synthesized recron reinforced silica aerogel blanket

77 K. Cumulative pore volume and pore size distributions (PSDs) were investigated by the BJH method. The comparative textural properties of synthesized pure silica aerogel and RSAB were tabulated in Table 1. Figure 4a illustrates the N_2 adsorption/desorption isotherms of pure silica aerogel and RSAB sample. Both the samples showed an adsorption/desorption curve with hysteresis behavior typical of aerogel, which indicates cylindrical pores, precisely analogous to supercritical/ambient pressure dried silica aerogel (H1 type) [31, 32]. The limited N_2 uptake at low relative pressures ($P/P_0 < 0.1$) indicates the existence of mesoporous structures [33]. The physisorption isotherms obtained for all aerogel samples exhibit hysteresis loops, which correspond to the characteristic features of mesoporous materials (Type IV isotherms) [32, 34]. The BET-specific surface area obtained for the RSAB sample (644 m^2/g) is less compared to the pure silica aerogel (1633 m^2/g). Figure 4b demonstrates the pore size distribution (PSDs) curves of pure and RSAB samples. The pore volume and pore size of RSAB is reduced due to the filler of recron fiber (pore diameter 17.13 nm) being less compared with the pure silica aerogel (pore diameter 19.21 nm) calculated from the BJH desorption isotherm.

Table 1 Effects of addition of recron fiber into silica aerogel matrix on the physical and textural properties of silica aerogel blanket

No	Sample name	Surface area (m^2/g) BET method	Density (g/cm^3)	Mean Pore diameter (nm)	Pore volume (cm^3/g) BJH method	Porosity (%)	Water absorption (ml/g)	Oil absorption (ml/g)	Moisture contents (%)
1	Pure silica aerogel (PSA)	1633	0.041	19.21	2.34	95	3.14	2.92	6
2	Reinforced silica aerogel blanket (RSAB)	644	0.09	17.13	1.37	87	0.135	3.74	9

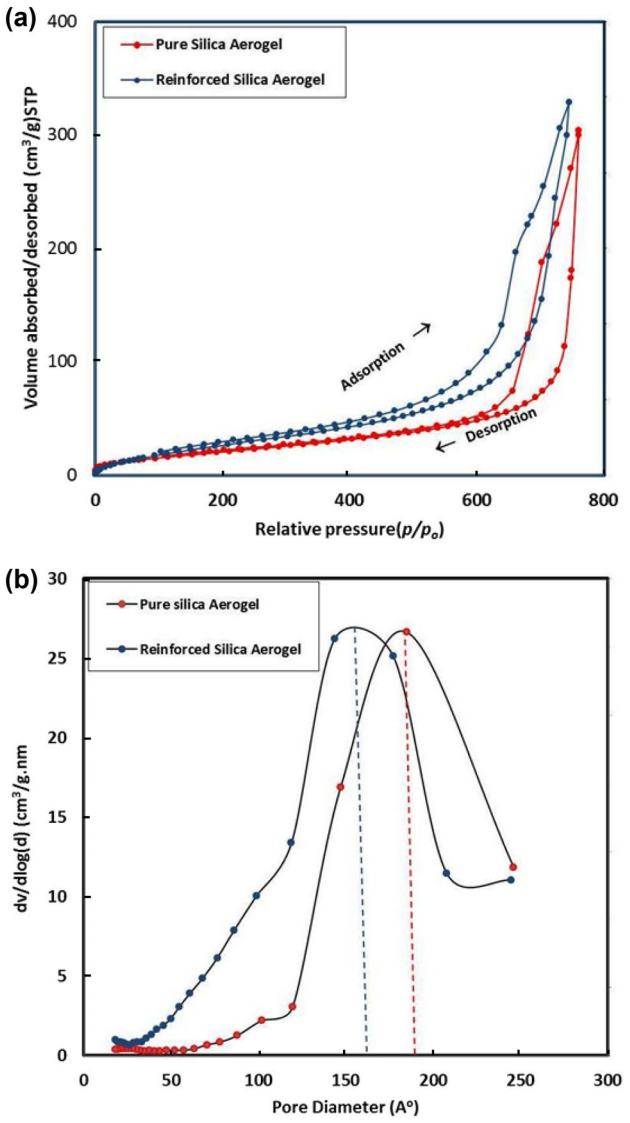

Fig. 4 **a** N_2 adsorption/desorption isotherms of pure silica and reinforced recron fiber silica aerogel blanket. **b** Pore size distributions of pure silica and reinforced recron fiber silica aerogel blanket (calculated from BJH desorption data)

Generally, in the silica aerogel, the pronounced peak lies in the mesoporous region (2–50 nm) [30]. The hysteresis loop indicates the desorption cycle of isotherms caused by the condensation implies the existence of the nanoporous during the drying process [35]. It confirms that silica aerogel matrix and porosity are preserved by reinforcing recron fiber even after drying the gel at an ambient pressure. The BJH adsorption indicates average pore diameter and pore volume of the flexible blanket is 17.13 nm and 1.37 cm^3/g. It can be seen from Table 1 that effect of addition of recron fiber in silica aerogel, the bulk densities (ρb) increased from 0.041 to 0.09 g/cm^3, while the porosity decreased from 95 to 87%, and the surface area decreased too from 1633 to 644 (m^2/g).

3.2 Microstructure properties of the silica aerogel blanket

The recron fibers of 10 µm size are dispersed in a disordered manner in a silica aerogel matrix having silica nanoporous particles. Figure 5a and b indicates the photographs of a synthesized pure silica aerogel and silica aerogel blanket respectively. The photographs of the RSAB sample are shown in Fig. 5b indicates the recron fiber is wrapped by silica aerogel particles. The microstructure of pure silica aerogel and silica aerogel blanket observed by scanning electron microscope is revealed in Fig. 6a & b (high and low magnification). Figure 6a indicates the 3-D highly porous network of the pure silica aerogel which reveals the nanostructured of the silica aerogel matrix. Figure 6b displays that the silica micronized grains appearing on the recron fibers look like spongy nature on the surface base. This resulted in change like the fibers as well as spread within nonwoven recron fiber interconnected with silica solid clusters acting as a backbone of the skeleton that could be accountable for the enhancement of mechanical strength and stiffness of silica aerogel blanket. The RSAB preserved a porous structure with relatively high porosity. The pore diameter (17.13 nm) is in the range of the mesoporous region (2–50 nm) [30]. Due to the miniature size of silica granules, interrupts are generated which causes a decline in thermal conductance and discontinuous spherical silica cluster with a three-dimensional silica network structure, resulting in the cut-off conveyance of heat [36].

3.3 Fourier transform infrared spectroscopy (FTIR) studies

Surface modification of aerogel blanket and pure silica aerogel was certified by a spectrum of fourier transform infrared spectroscopy (FTIR). The aerogel samples were made into powders and mixed with KBr then pressed to form a sample disk for FTIR result. Figure 7 of the FT-IR spectra indicate the chemical bonding of pure and reinforced silica aerogel prepared by APD. It can be observed that the stretching and bending vibration of broad spectra at 3450 cm^{-1} is due to the presence of the residual –OH groups, which indicates a more hydrophobic nature which has been confirmed with measurement of the angle of contact [37]. The peaks at around 1630 cm^{-1} indicate stretching vibrations of ≡Si–OH group formed due to the unreacted Si–OH of the sodium silicate [38]. The absorption peaks at 2890 and 840 cm^{-1} relate to the Si–C vibration and the presence of C–H vibrations can be seen $–CH_3$ terminal group which points to the surface modification of blanket successfully done with surface modification agent TMCS properly [39]. The peaks of the 1070 and 495 cm^{-1} band denote the adsorption peaks of the Si–O–Si vibrations. The hydrophobicity of the silica aerogel blanket was also certified with the help of water droplets put on the

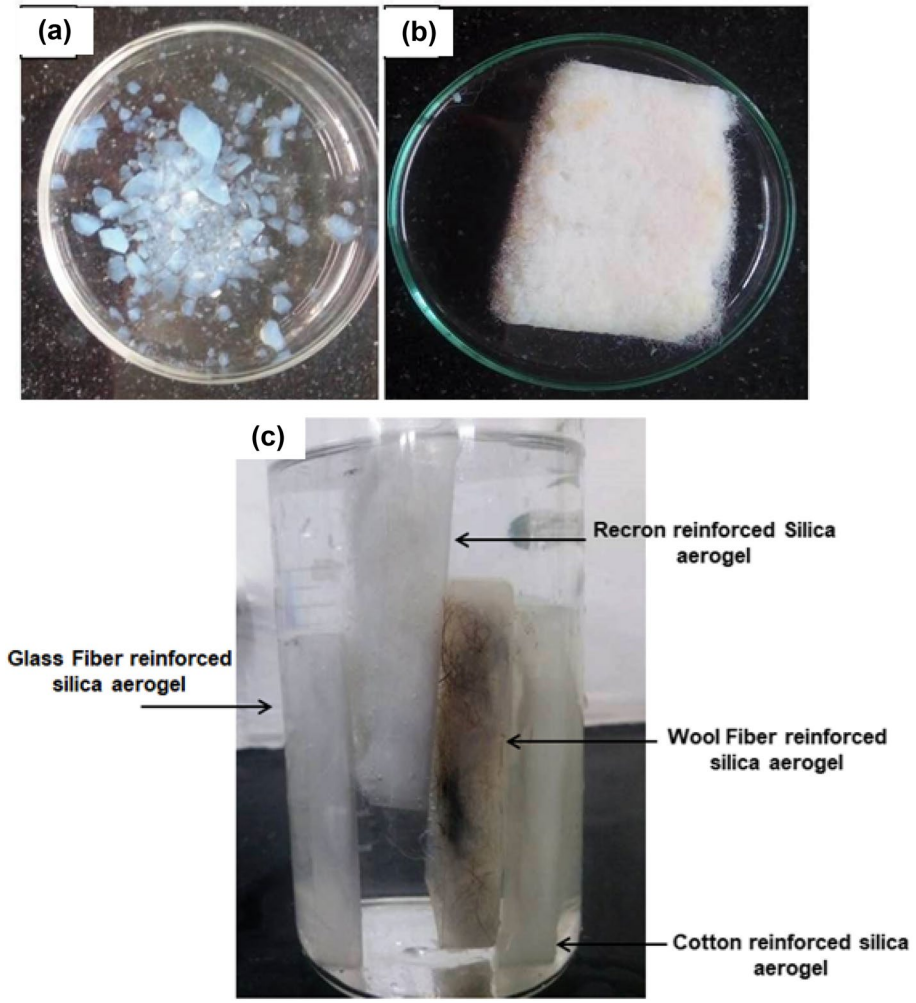

Fig. 5 Photographs of **a** pure silica aerogel, **b** silica aerogel with reinforced recron fiber and **c** Photograph showing light weight recron fiber reinforced silica aerogel sheet floating in water compared to glass fiber, wool fiber and cotton reinforced silica aerogels

surface of the silica blanket which is represented in Fig. 8. This confirms the hydroxyl groups (–OH) are successfully replaced by hydrophobic methyl groups ($–CH_3$) which are signified by surface modification reactions. According to the positions of the distinctive bands, it is detected that the critical point could be at 270 °C by following the intensity of peaks corresponding to Si-CH_3, C–H and Si–OH groups. Due to that the thermal stability of the final aerogel blanket could be up to 270 °C and the hydrophobicity could vanish above this temperature.

3.4 Hydrophobic nature of the monolithic silica aerogel blanket

Figure 8 illustrates the hydrophobic nature of RSAB was measured with the help of contact angle measurement. Water (0.01 mL) was utilized to form a water droplet on a silica aerogel blanket surface which was captured by a high-resolution camera along with a bifocal lens used to enlarge the image of the tiny nature of the water droplet. The water droplet was floating on the surface of the silica aerogel blanket; means not stable at one place indicates the existence of a stable methyl group in charge of the hydrophobic feature of the silica aerogel blanket. The blanket sample indicates a superhydrophobic nature of contact angle of > 120°.

The oil absorption capacity mentioned in Table 1 and calculated with the equation [40, 41] as follows:

$$Q(\%) = [W - W_o/\rho LV_o] \times 100 \quad (2)$$

W and W_o are the weights of Aerogels before and after absorption respectively. V_o = the volume of aerogel.

The percentage of moisture content ω (m/m %) of the material [42] revealed in Table 1 and intended by given formula:

$$\omega\ (m/m\%) = (M_{wet} - M_{dry})/M_{dry} \times 100 \quad (3)$$

where, M_{wet} and M_{dry} are the mass of the wet and dry RSAB sample respectively.

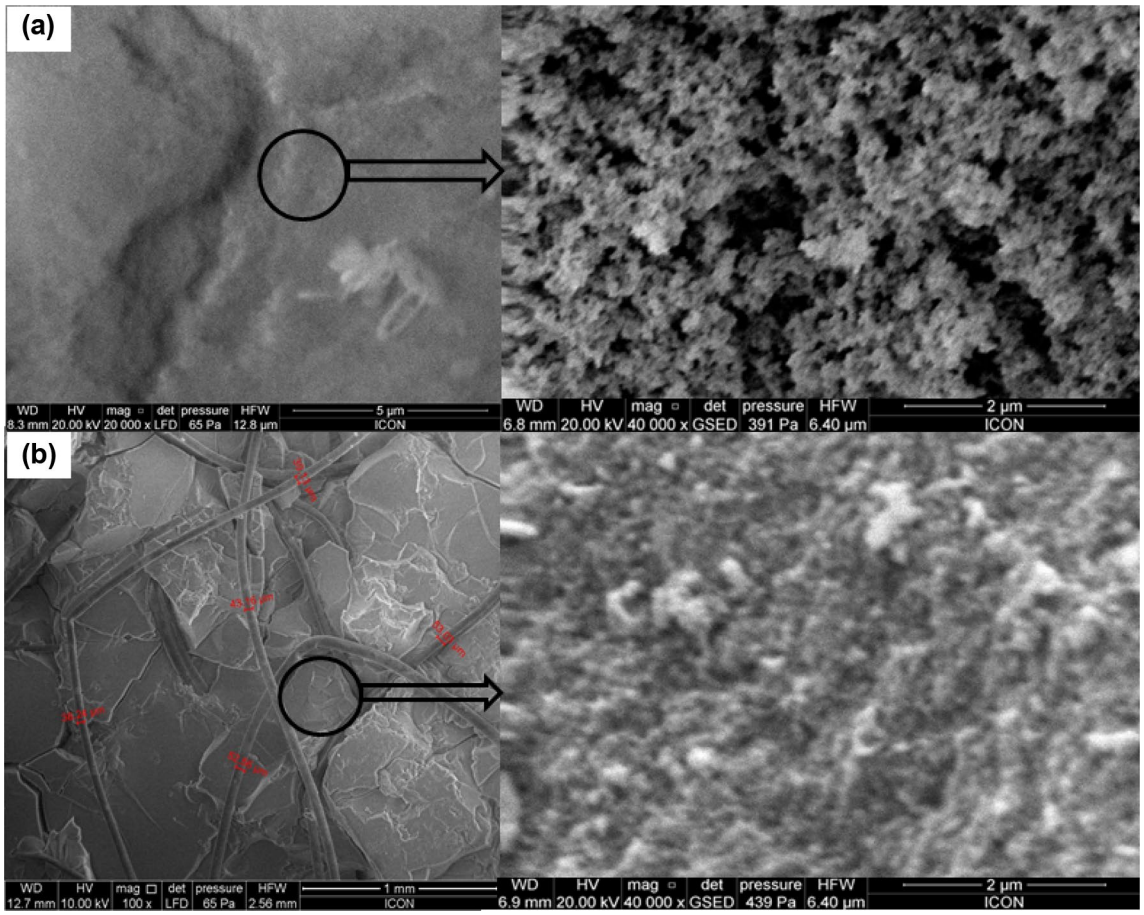

Fig. 6 SEM micrographs of (low & high magnification) **a** pure silica aerogel and **b** silica aerogel composites with reinforced recron fiber

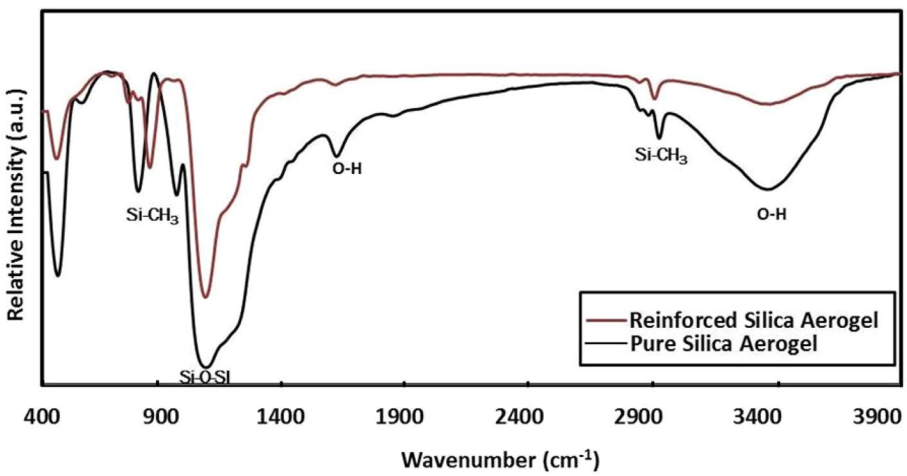

Fig. 7 FTIR spectra of **a** pure silica aerogel and **b** silica aerogel composites with reinforced recron fiber

3.5 Thermal stability of the silica aerogel blanket

Figure 9 indicates the thermal stability of the silica aerogel blanket has been investigated by using thermogravimetric and differential thermal analysis (TG–DTA). The pure silica aerogel and the silica aerogel blanket were kept in the furnace at different increasing temperatures. The thermal decomposition of each sample takes place in a programmed temperature range of 25–1000 °C. In the case of RSAB at the starting point, insignificant weight loss was detected between 25 and 70 °C which was due to the vaporization of humidity absorbed by the aerogel blanket. The weight loss

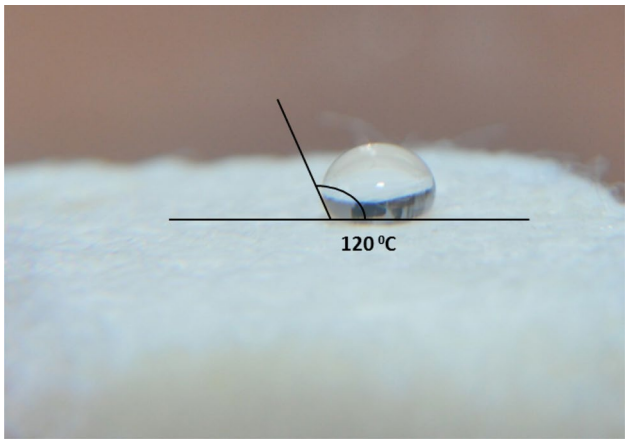

Fig. 8 Contact angle of silica aerogel composites with reinforced recron fiber

at the temperature after 270 °C was due to the oxidation of Si–CH_3 groups on the RSAB surface, which indicated the first exothermic peak [43]. The TGA curve constantly decreases owing to the rapid oxidation of methyl groups (CH_3) and disintegration of organic polymeric chains [34]. The curves represent the minor weight loss up to a temperature of 400 °C of silica aerogel blanket. Figure 9 exhibits the hydrophobic nature of pure silica aerogel and the aerogel blanket was retained up to 400 °C. Over temperature, they demonstrate the hydrophilic nature attributable to the oxidation of surface methyl groups (–CH_3). It was distinctly illustrated with an abrupt change in exothermic peaks remarkable in DTA curves as boost up to a temperature above 400 °C and 270 °C in pure silica and silica aerogel blankets respectively, for the authorization of oxidation of surface methyl groups and decomposition of the organic molecule [44]. The thermogravimetric and differential thermal analysis indicates that the pure silica aerogel demonstrates more weight loss after 420 °C compared to the silica aerogel blanket, which indicates better thermal stability for RSAB at a higher temperature.

Furthermore, the thermal conductivity of the silica aerogel blankets were investigated by using differential scanning calorimetry (DSC). The DSC plots of pure and reinforced silica aerogel e.g., variation of heat flow and heat capacity as a function of temperature, are illustrated in Fig. 10. Nitrogen gas was utilized at a rate of 50 mL/min to expel gas for DSC measurement. The specimen of 6.89 mg (pure silica aerogel) and 4.94 mg (RSAB) of the samples were put in an aluminum crucible and closed by pressing an aluminum lid which was pierced by a needle on the top for degassing. The samples were heated from ambient temperature to 1000 °C at a heating rate of 10 °C/min. The thermal conductivity (k) of reinforced recron fiber silica aerogel blanket was calculated from the analysis of the DSC curves while heating by using the following relation [45, 46].

$$k = qL/A(T_h - T_l)W/cm\ ^\circ C \quad (4)$$

where q is the heat flow, L is the thickness, A is the area, (T_h –T_l) is the difference between high and low temperature.

The discrepancy of the thermal conductivity k of pure silica aerogel and silica aerogel blanket (RSAB) is depicted in Fig. 10. In Fig. 10, it has been observed that the thermograms of pure silica and reinforced recron fiber silica blanket which show initial endothermic peaks (T_d) at 70 °C and

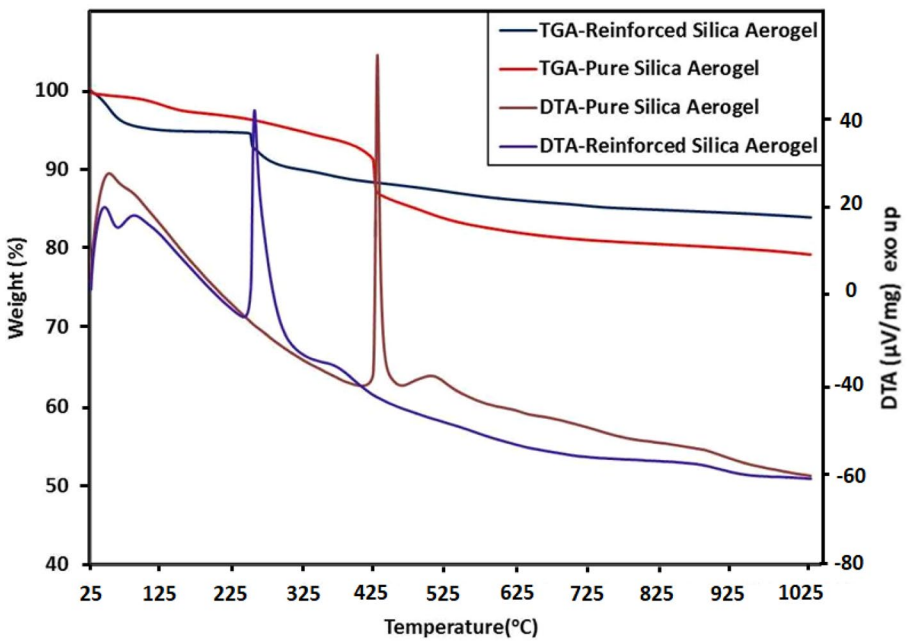

Fig. 9 TG/DTA curves of **a** pure silica aerogel and **b** silica aerogel composites with reinforced recron fiber (heating rate 10 °C/min)

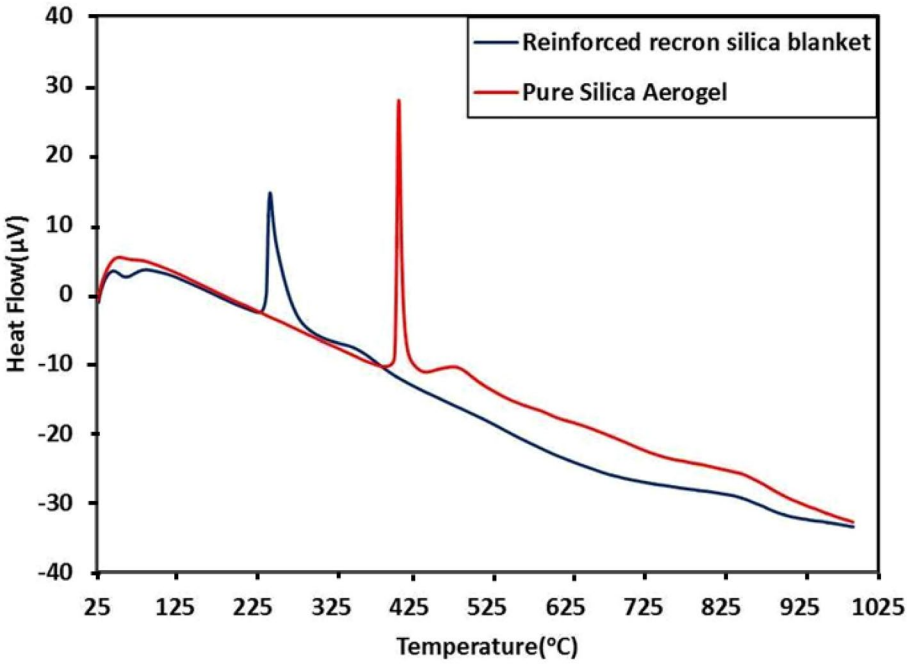

Fig. 10 DSC curves of **a** pure silica aerogel and **b** silica aerogel composites with reinforced recron fiber (heating rate 10 °C/min.)

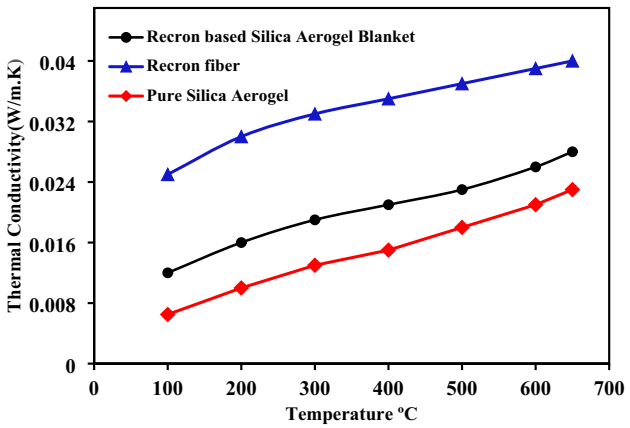

Fig. 11 Thermal conductivity of bare fiber, RSAB and pure silica aerogel with different temperatures

50 °C and higher exothermic peaks at 410 °C and 246 °C, respectively. The DSC analysis indicates that recron blankets can be used safely up to 246 °C. Endothermic peaks (T_d) correspond to increasing hydrophobic groups of silica aerogel nanoparticles content with the loss of water [47] while hydrophobic groups are replaced by hydrophilic groups of silica aerogel during exothermic peaks. It indicates that thermal conductivity diminishes with the accumulation of recron fiber due to the disturbance of heat transfer within a bunch of silica granules networks.

Figure 11 depicts the thermal conductivities of the recron fiber, RSAB, and pure silica aerogel. It can be observed that the thermal conductivity of the as prepared RSAB samples had a minute variation from with addition of 3 wt.% recron fibers. The heat transfers through the material through 3 mechanisms such as the gaseous conductivity, solid conductivity, and radiative transmission through pores. The resultant thermal conductivity of the insulating material is expressed as [40, 48].

$$\lambda_e = \lambda_c + \lambda_r \tag{5}$$

where, the λ_e is the effective thermal conductivity of insulating material, the λ_c the sum of the gaseous thermal conductivity and solid thermal conductivity, and the λ_r is thermal conductivity related to the radiative transmission.

The Silica aerogel blanket could restrict gas conduction, due to nano-particles interconnected in a 3D matrix. Gaseous conductivity diminishes due to the nanoporous structure which restricts the mean free path of gas. The solid conduction of heat transfer directly depends on the porosity and density. In RSAB, fiber content in silica aerogel reduces the radiative conductivity of nanocomposite due to increased density of introduced fiber content. Therefore, the thermal conductivity of RSAB nanocomposite decreases in comparison to the pure silica aerogel. When the 3 wt.% recron fibers added in silica sol, the thermal conductivity of the RSAB decreased at ambient temperature. Recron fibers doped nanocomposite improve the solid thermal conductivity. However, diminish the radiative conductivity, and the thermal conductivity of RSAB at room temperature. In comparison to pure silica aerogel, RSAB shows increased thermal conductivity due to the solid backbone of recron fibers.

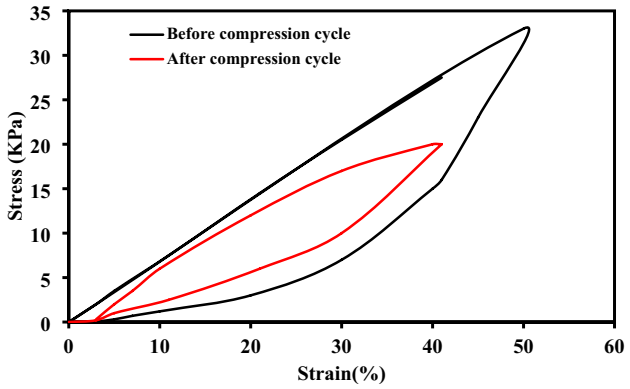

Fig. 12 The uniaxial compression test of stress–strain curve of RSAB nanocomposites

3.6 Mechanical strength

The flexibility of RSAB nanocomposite is also described by the universal testing machine (Fig. 12). The comparative thermal and mechanical, of the recron fiber-reinforced aerogels with other fibered reinforced aerogels were tabulated in Table 2. The RSAB can be repetitively compressed at 60% strain for 30 cycles without destruction the structure, indicating the superior mechanical strength of the RSAB. The strain is fixed at 60%, and the applied maximum stress is around 15 kPa before cycle, indicate low value of Young's modulus and good elasticity. The stress is slightly reduced to 14 kPa after 30 compression test cycle. We explored the mechanical strength of the RSAB through uniaxial compression test under various strains. In Fig. 12, after compression test, the as-prepared RSAB can regain its original shape. RSAB nanocomposite shows superb elasticity under 60% strain can be applicable for commercial insulating materials in several fields of applications.

4 Conclusion

The effect of simulated electrical home appliances on the properties of RSAB has been investigated. It has been revealed that the thermal insulation execution was unaffected by thermal stability tests of aerogels for the conservation of energy in electrical appliances. The embedding of recron fibers significantly affects the resistance of the silica aerogel to overcome the fragility of the silica aerogel, an ambient pressure drying technique with help of industrial-grade cheap sodium silicate precursor. The major issue of lightweight feature collapse in the case of maintaining monolithic structure with the help of reinforcement of additives in pure silica nanostructure is preserved due to low-density recron fiber. Not only was a significant increase of the flexibility of the silica matrix, but also improved the thermal resistance, stiffness and monolithic structure was achieved with reasonable specific surface area and pore diameter of 644 m^2/g and 17.13 nm respectively at an optimal range. TG–DTA analysis indicates that the hydrophobicity is preserved up to the 380 °C of the recron reinforced silica aerogel blanket. The contact angle (120°) of the silica aerogel blanket shows the hydrophobic nature of the sample. The presence of CH_3 groups in FTIR spectra indicates the surface modification was successfully done for the silica aerogel blanket. The recent approach is more economical and safe to manufacture silica aerogel blankets for large-scale industrial production. The flexible silica aerogel exhibits an excellent thermal insulation property and better thermal stability, flexibility, outstanding comprehensive strength, and hydrophobic nanocomposite would be a novel nanoporous material for thermal insulating material widespread commercial applications.

Table 2 Comparison of thermal and mechanical properties of the recron fiber-reinforced aerogels with other fibered reinforced aerogels

No	Silica aerogel composites	Thermal conductivity (W/m K)	Young's modulus	References
1	Glass fiber (2.5%)	0.0258	750 kPa	[14]
2	Xonotlite fiber (XF)	0.0285	–	[16]
3	Aramid fiber	0.026	350 kPa	[49]
4	Aramid fibrid/mica (AM),	–	11.6 MPa	[50]
5	Aramid fibrid/nanofibrillated cellulose (AN)	–	22.1 MPa	
6	Mica/nanofibrillated cellulose (MN)	–	34.6 MPa	
7	SiO_2-SSNF-3%	0.025	70 kPa	[51]
8	Recron fiber (3%)	0.028	34 kPa	This work

Acknowledgements The authors gratefully acknowledge the University of Mumbai under a minor research project, Department of Physics and University of Jeddah, Deanship of Scientific Research (DSR) under the research project grant (UJ-02-020-ICGR), and DST-SERB project grant (EEQ/2020/0002980) for their technical and financial support.

Author contributions All authors contributed equally.

Funding The authors have not disclosed any funding.

Data availability Yes.

Code availability Not applicable.

Declarations

Conflict of interest The authors declare that they have no conflict of interest.

References

1. H.J. Zhan, K.J. Wu, Y.L. Hu, J.W. Liu, H. Li, X. Guo et al., Biomimetic carbon tube aerogel enables super-elasticity and thermal insulation. Chem **5**, 1871–1882 (2019)
2. T. Chen, C. Liu, P. Mu, H. Sun, Z. Zhu, W. Liang, A. Li, Fatty amines/graphene sponge form-stable phase change material composites with exceptionally high loading rates and energy density for thermal energy storage. Chem. Eng. J. **382**, 122831 (2020)
3. Z.L. Yu, N. Yang, V. Apostolopoulou-Kalkavoura, B. Qin, Z.Y. Ma, W.Y. Xing et al., Fire-retardant and thermally insulating phenolic-silica aerogels. Angew. Chem. Int. Ed. **57**, 4538–4542 (2018)
4. S. He, Y. Huang, G. Chen, M. Feng, H. Dai, B. Yuan, X. Chen, Effect of heat treatment on hydrophobic silica aerogel. J. Hazard. Mater. **362**, 294–302 (2019)
5. W.C. Hung, R.S. Horng, R.E. Shia, Investigation of thermal insulation performance of glass/carbon-fiber-reinforced silica aerogel composites. J. Sol-Gel. Sci. Technol. **97**, 414–421 (2021)
6. Y.F. Lin, Y.J. Lin, C.C. Lee, K.Y.A. Lin, T.W. Chung, K.L. Tung, and Synthesis of mechanically robust epoxy cross-linked silica aerogel membranes for CO_2 capture. J. Taiwan Inst. Chem. Eng. **87**, 117–122 (2018)
7. Y. Zhang, L. Xiang, Q. Shen, X. Li, T. Wu, J. Zhang, C. Nie, Rapid synthesis of dual-mesoporous silica aerogel with excellent adsorption capacity and ultra-low thermal conductivity. J. Non-Cryst. Solids **555**, 120547 (2021)
8. H. Rocha, U. Lafont, C. Semprimoschnig, Environmental testing and characterization of fibre reinforced silica aerogel materials for mars exploration. Acta Astronaut. **165**, 9–16 (2019)
9. D.J. Boday, P.Y. Keng, B. Muriithi, J. Pyun, D.A. Loy, Mechanically reinforced silica aerogel nanocomposites via surface initiated atom transfer radical polymerizations. J. Mater. Chem. **20**, 6863–6865 (2010)
10. S. Iswar, W.J. Malfait, S. Balog, F. Winnefeld, M. Lattuada, M.M. Koebel, Effect of aging on silica aerogel properties. Microporous Mesoporous Mater. **241**, 293–302 (2017)
11. M.A. Einarsrud, E. Nilsen, A. Rigacci, G.M. Pajonk, S. Buathier, D. Valette et al., Strengthening of silica gels and aerogels by washing and aging processes. J. Non-Cryst. Solids **285**, 1–7 (2001)
12. T.Y. Wei, S.Y. Lu, Y.C. Chang, A new class of opacified monolithic aerogels of ultralow high-temperature thermal conductivities. J. Phys. Chem. C **113**, 7424–7428 (2009)
13. L. Yan, H. Ren, J. Zhu, Y. Bi, L. Zhang, One-step eco-friendly fabrication of classically monolithic silica aerogels via water solvent system and ambient pressure drying. J. Porous Mater. **26**, 785–791 (2019)
14. S. Shafi, Y. Zhao, Superhydrophobic, enhanced strength and thermal insulation silica aerogel/glass fiber felt based on methyltrimethoxysilane precursor and silica gel impregnation. J. Porous Mater. **27**, 495–502 (2020)
15. Y. Huang, S. He, G. Chen, H. Dai, B. Yuan, X. Chen, X. Yang, Fast preparation of glass fiber/silica aerogel blanket in ethanol & water solvent system. J. Non-Cryst. Solids **505**, 286–291 (2019)
16. M. Li, H. Jiang, D. Xu, Synthesis and characterization of a xonotlite fibers–silica aerogel composite by ambient pressure drying. J. Porous Mater. **25**, 1417–1425 (2018)
17. D. Du, Y. Jiang, J. Feng, L. Li, J. Feng, Facile synthesis of silica aerogel composites via ambient-pressure drying without surface modification or solvent exchange. Vacuum **173**, 109117 (2020)
18. A. Darmawan, S.A. Rasyid, Y. Astuti, Modification of the glass surface with hydrophobic silica thin layers using tetraethylorthosilicate (TEOS) and trimethylchlorosilane (TMCS) precursors. Surf. Interface Anal. **53**, 305–313 (2020)
19. C. Li, X. Cheng, Z. Li, Y. Pan, Y. Huang, L. Gong, Mechanical, thermal and flammability properties of glass fiber film/silica aerogel composites. J. Non-Cryst. Solids **457**, 52–59 (2017)
20. M. Ramamoorthy, A.A. Pisal, R.S. Rengasamy, A.V. Rao, In-situ synthesis of silica aerogel in polyethylene terephthalate fibre nonwovens and their composite properties on acoustical absorption behavior. J. Porous Mater. **25**, 179–187 (2018)
21. P. Liu, H. Gao, X. Chen, D. Chen, J. Lv, M. Han, G. Wang, In situ one-step construction of monolithic silica aerogel-based composite phase change materials for thermal protection. Compos. B: Eng. **195**, 1072 (2020)
22. H. Cheng, Z. Fan, C. Hong, X. Zhang, Lightweight multiscale hybrid carbon-quartz fiber fabric reinforced phenolic-silica aerogel nanocomposite for high temperature thermal protection. Compos. A: Appl. Sci. Manuf. **143**, 1313 (2021)
23. M.R. Bhuiyan, L. Wang, A. Shaid, I. Jahan, R.A. Shanks, Silica aerogel-integrated nonwoven protective fabrics for chemical and thermal protection and thermophysiological wear comfort. J. Mater. Sci. **55**, 2405–2418 (2020)
24. Dong Zhang, *Advances in filament yarn spinning of textiles and polymers* (WpWoodhead Publishing, Sawston, 2014)
25. Z.A.A. Halim, M.A.M. Yajid, H. Hamdan, Effects of solvent exchange period and heat treatment on physical and chemical properties of rice husk derived silica aerogels. Silicon **13**, 251–257 (2021)
26. S. Yue, X. Li, H. Yu, Z. Tong, Z. Liu, Preparation of high-strength silica aerogels by two-step surface modification via ambient pressure drying. J. Porous Mater. **28**, 651–659 (2021)
27. C. Zhao, Y. Li, W. Ye, X. Shen, X. Yuan, C. Ma, Y. Cao, Performance regulation of silica aerogel powder synthesized by a two-step sol-gel process with a fast ambient pressure drying route. J. Non-Cryst. Solids **567**, 120923 (2021)
28. P.B. Sarawade, J.K. Kim, H.K. Kim, H.T. Kim, High specific surface area TEOS-based aerogels with large pore volume prepared at an ambient pressure. Appl. Surf. Sci. **254**, 574–579 (2007)
29. S. Shafi, R. Navik, X. Ding, Y. Zhao, Improved heat insulation and mechanical properties of silica aerogel/glass fiber composite by impregnating silica gel. J. Non-Cryst. Solids **503**, 78–83 (2019)
30. M. Cai, S. Shafi, Y. Zhao, Preparation of compressible silica aerogel reinforced by bacterial cellulose using tetraethylorthosilicate and methyltrimethoxylsilane co-precursor. J. Non-Cryst. Solids **481**, 622–626 (2018)

31. P.B. Sarawade, J.K. Kim, A. Hilonga, D.V. Quang, H.T. Kim, Synthesis of hydrophilic and hydrophobic xerogels with superior properties using sodium silicate. Microporous Mesoporous Mater. **139**, 138–147 (2011)
32. L. López-Pérez, V. Zarubina, I. Melián-Cabrera, The Brunauer–Emmett–Teller model on alumino-silicate mesoporous materials. How far is it from the true surface area. Microporous Mesoporous Mater. **319**, 1065 (2021)
33. S. Cui, S. Yu, B. Lin, X. Shen, X. Zhang, D. Gu, Preparation of amine-modified SiO_2 aerogel from rice husk ash for CO 2 adsorption. J. Porous Mater. **24**, 455–461 (2017)
34. N. Marinkov, M. Markova-Velichkova, S. Gyurov, Y. Kostova, I. Spassova, D. Rabadjieva, G. Gentscheva, Preparation and characterization of silica gel from silicate solution obtained by autoclave treatment of copper slag. J. Sol-Gel. Sci. Technol. **87**, 331–339 (2018)
35. P.B. Sarawade, J.K. Kim, A. Hilonga, H.T. Kim, Production of low-density sodium silicate-based hydrophobic silica aerogel beads by a novel fast gelation process and ambient pressure drying process. Solid State Sci. **12**, 911–918 (2010)
36. W.J. Schmitt, *The preparation and properties of acid-catalyzed silica aerogel* (The University of Wisconsin-Madison, Madison, 1982)
37. J. Chen, B. Zhang, M.Q. Wei, J. Men, G.W. Miao, The optimum of preparation and characterization of aerogels like hydrophobic titania by ambient pressure drying. Adv. Mater. Res. **1120**, 264–274 (2015)
38. H. Krishna, M.O. Haus, R. Palkovits, Basic silica catalysts for the efficient dehydration of biomass-derived compounds–elucidating structure-activity relationships for Na2O/SiO2-type materials. Appl. Catal. B: Environ. **286**, 119933 (2021)
39. L.J. Wang, S.Y. Zhao, M. Yang, Structural characteristics and thermal conductivity of ambient pressure dried silica aerogels with one-step solvent exchange/surface modification. Mater. Chem. Phys. **113**, 485–490 (2009)
40. M. Wang, N. Pan, Predictions of effective physical properties of complex multiphase materials. Mater. Sci. R. **63**, 1–30 (2008)
41. S.D. Doke, C.M. Patel, V.N. Lad, Improving physical properties of silica aerogel using compatible additives. Chem. Pap. **75**, 215–225 (2021)
42. Á. Lakatos, Stability investigations of the thermal insulating performance of aerogel blanket. Energy Build. **185**, 103–111 (2019)
43. T. Zhou, X. Cheng, Y. Pan, C. Li, L. Gong, H. Zhang, Mechanical performance and thermal stability of glass fiber reinforced silica aerogel composites based on co-precursor method by freeze drying. Appl. Surf. Sci. **437**, 321–328 (2018)
44. Y.K. Lee, V.G. Parale, H.H. Cho, D.B. Mahadik, H.H. Park, Hydrophobic silica composite aerogels using poly (methyl methacrylate) by rapid supercritical extraction process. J. Sol-Gel. Sci. Technol. **83**, 692–697 (2017)
45. C.P. Camirand, Measurement of thermal conductivity by differential scanning calorimetry. Thermochim. Acta **417**(1), 1–4 (2004)
46. S. Knhasamy, A. Store, G.M. Haarberg, S. Kjelstrup, A. Solheim, Thermal conductivity of molten carbonates with dispersed solid oxide from differential scanning calorimetry. Materials **12**(9), 1486 (2019)
47. Z. Li, X. Cheng, L. Gong, Q. Liu, S. Li, Enhanced flame retardancy of hydrophobic silica aerogels by using sodium silicate as precursor and phosphoric acid as catalyst. J. Non-Cryst. Solids **481**, 267–275 (2018)
48. X.B. Hou, R.B. Zhang, D.N. Fang, Novel whisker-reinforced Al_2O_3- SiO_2 aerogel composites with ultra-low thermal conductivity. Ceram. Int. **43**, 9547–51 (2017)
49. Z. Li, X. Cheng, S. He, X. Shi, L. Gong, H. Zhang, Aramid fibers reinforced silica aerogel composites with low thermal conductivity and improved mechanical performance. Compos. A Appl. Sci. Manuf. **84**, 316–325 (2016)
50. Z. Lu, D. Ning, W. Dang, D. Wang, F. Jia, J. Li, E. Songfeng, Comparative study on the mechanical and dielectric properties of aramid fibrid, mica and nanofibrillated cellulose based binary composites. Cellulose **27**, 8027–8037 (2020)
51. R. Zhang, Z. An, Y. Zhao, L. Zhang, P. Zhou, Nanofibers reinforced silica aerogel composites having flexibility and ultra-low thermal conductivity. Int. J. Appl. Ceram. Technol. **17**, 1531–1539 (2020)